# COMPARISON OF CLASSICAL AND QUANTUM PHASE SPACE STRUCTURE OF NONRIGID MOLECULES, LiCN

R.M. BENITO [1], F. BORONDO [2], J.-H. KIM, B.G. SUMPTER [3] and G.S. EZRA [4]
*Department of Chemistry, Baker Laboratory, Cornell University, Ithaca, NY 14853, USA*

Received 25 April 1989; in final form 7 July 1989

We examine the classical and quantum phase space structure of the nonrigid molecule LiCN. The quantum phase space density for many vibrational eigenstates exhibits marked localization in classically chaotic regions of phase space.

## 1. Introduction

There has been much recent progress in understanding the classical phase space structure of nonintegrable two-mode coupled oscillator systems and associated area-preserving mappings [1]. The important role of phase space features such as cantori [2,3] and partial separatrices [4,5] as bottlenecks in intramolecular energy transfer [6], isomerization [7], unimolecular decay [8–10], and bimolecular reactions [11,12] has been demonstrated. Two major problems are currently outstanding. The first concerns the generalization of theories of transport based on phase space bottlenecks [2,6,13] to multimode classical systems [14–17]. The second concerns the relation between the classical and quantum phase space structure of nonintegrable systems [18,19]. The present paper addresses the second problem.

Recent work has revealed a striking localization of quantum eigenstates in both configuration space [20] and phase space [19,21–27] for many systems, even in regions of phase space that are classically quite chaotic. Unstable periodic orbits have been found to influence the form of individual eigenstates in an as yet incompletely understood fashion [19–30], while quantum phase space densities trapped by classical cantori [21,23] and localized along separatrix manifolds [19,22,24,27] have been observed.

In this Letter we compared the classical and quantum phase space structure of a two-mode model of the nonrigid molecule LiNC/LiCN, in which the CN bond is frozen. The LiCN molecule has served as a test case for quantum mechanical methods for calculation of vibration–rotation levels in floppy systems [31,32]. An ab initio potential surface (see fig. 1) is available [33].

An earlier comparative study of the classical and quantum mechanics of two-mode LiCN has been made by Farantos and Tennyson (FT) [31]. By examining configuration space plots of the first 80 (rotationless) eigenstates of LiCN, FT classified the vibrational states into 5 different types: regular states localized around the LiNC minimum; irregular states localized around the LiNC minimum; regular states localized around LiCN; irregular, delocalized states; and free rotor or "polytopic" states. The regularity or otherwise of an eigenstate was judged by the complexity of its nodal pattern [34]. Other previously proposed diagnostics of "quantum chaos" such as level spacing statistics [35], sensitivity of eigenvalues to changes in the Hamiltonian [36], and avoided crossings of energy levels [37] were also studied. Corresponding studies of surfaces of section [1] and

[1] Permanent address: Departamento de Fisica, ETSI Telecomunicacion, Politecnica University, 28040 Madrid, Spain.
[2] Permanent address: Departamento Quimica C-14, Universidad Autonoma de Madrid, Cantoblanco, 28049 Madrid, Spain.
[3] Permanent address: Chemistry Division, Oak Ridge National Laboratory, Oak Ridge, TN 37831, USA.
[4] Alfred P. Sloan Fellow; Camille and Henry Dreyfus Teacher-Scholar.



0 009-2614/89/$ 03.50 

$K$-entropies [38] for classical trajectories were also made, and revealed the early onset of widespread nonquasiperiodic motion. FT concluded that there is an early onset of "quantum chaos" in LiCN, and that there is good qualitative agreement between quantum and classical mechanics for LiCN, albeit with some "quantum sluggishness".

In the present paper we examine both the classical and quantum mechanics of LiCN on the same footing, i.e. in phase space. There is found to be marked localization of quantum phase space density in apparently highly chaotic regions of classical phase space. Such a finding is in accord with recent work on the quantum/classical correspondence for other systems [19–27]; the present study extends these findings to a realistic model of the highly nonrigid molecule LiCN.

## 2. Classical mechanics of LiNC/LiCN

Elucidation of the classical and quantum phase space structure of the nonrigid molecule LiCN involves several technical difficulties, as discussed in detail elsewhere [39]. For present purposes, we briefly outline the method used to study the classical dynamics of LiCN in this section, and the corresponding quantum calculation in section 3.

The potential surface used for LiCN is that of ref. [33], expressed in scattering coordinates ($R$, $\theta$):

$$V(R,\theta)=\sum_{\lambda=0}^{9} P_\lambda(\cos\theta)\, V_\lambda(R)\,. \qquad (1)$$

$R$ is the distance from Li to the center of mass of CN, $\theta$ is the angle between the CN axis and the Li to CN vector, and $P_\lambda$ is the Legendre polynomial of order $\lambda$. The potential is a sum of short-range and long-range parts, with coefficients $V_\lambda$ as a function of $R$ given in ref. [33].

A contour plot of the potential surface is shown in fig. 1. The existence of minima at the linear configurations LiNC and LiCN should be noted; the energy difference $E(\mathrm{LiCN})-E(\mathrm{LiNC})=2281\ \mathrm{cm}^{-1}$. The minimum energy path $R_e(\theta)$ connecting the two isomers is shown as a dotted curve. We have fitted the minimum energy path $R_e(\theta)$ to a series in $\cos\theta$:

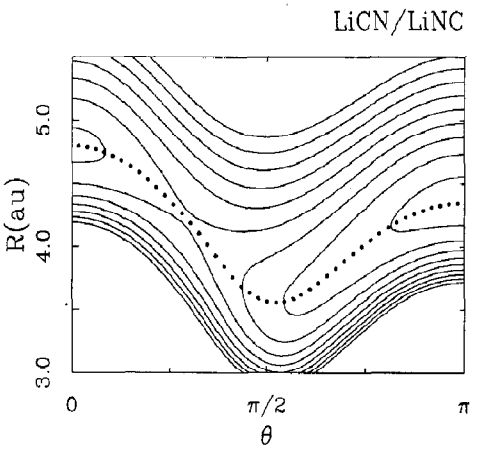


Fig. 1. Contour plot of the potential energy surface for LiCN/LiNC of ref. [33]. $R$ is given in atomic units. $\theta=0$ corresponds to the LiCN minimum, $\theta=\pi$ to LiNC. The minimum energy path connecting the two isomers is shown as a dotted line (cf. eq. (2)).

$$R_e(\theta)=4.1159+0.2551\cos\theta+0.4983\cos 2\theta +0.05343\cos 3\theta-0.068124\cos 4\theta +0.020578\cos 5\theta\,, \qquad (2)$$

in atomic units. The height of the LiNC/LiCN barrier is 3454 $\mathrm{cm}^{-1}$. LiCN is a very nonrigid molecule, capable of complicated internal motions. At relatively modest energies, the system can pass between the two isomeric forms, with the Li orbiting around the CN [31,39].

The classical Hamiltonian for rotationless LiCN is

$$H=p_R^2/2\mu_1+\tfrac{1}{2}(1/\mu_1R^2+1/\mu_2r^2)p_\theta^2+V(R,\theta)\,, \qquad (3)$$

where $p_R$ and $p_\theta$ are the momenta conjugate to $R$ and $\theta$, respectively, $\mu_1$ is the Li–CN reduced mass, $\mu_2$ is the reduced mass of CN, and $r$ is the CN bond length, frozen at its equilibrium value 2.186 bohr [31].

The surface of section (SOS) [1] is used to study the classical phase space structure of two-mode LiCN. A very useful choice of SOS is defined by taking the sectioning coordinate to lie along the minimum energy path connecting LiNC and LiCN. That is, the values of the coordinate ($p_\theta$, $\theta$) are noted every time that a trajectory has $R=R_e(\theta)$. To ensure that the SOS is an area-preserving map [1], it is necessary to make a canonical transformation $(R,\theta,p_R,p_\theta)\rightarrow(\rho,$

$\psi$, $p_\rho$, $p_\psi$), with generating function [39]

$$F(R, \theta, p_\rho, p_\psi) = p_\rho[R - R_e(\theta)] + p_\psi\theta . \quad (4)$$

The generating function (4) is of the $F_2$ type [1], i.e. a function of the old coordinates and the new momenta. The new coordinates ($\rho$, $\psi$) are obtained in terms of ($R$, $\theta$, $p_\rho$, $p_\psi$) by differentiation of $F$ with respect to the momenta ($p_\rho$, $p_\psi$), while the old momenta ($p_R$, $p_\theta$) are obtained by differentiation with respect to ($R$, $\theta$). The coordinate $\rho$ describes displacements transverse to the minimum energy path.

The SOS used here is then a plot of the conjugate pair of variables ($\psi$, $p_\psi$) at every intersection of the trajectory with the reaction coordinate, where $\rho = 0$ (i.e. $R = R_e(\psi)$), and $p_\rho$ is chosen to be on a particular branch of the momentum. The quantum wavefunctions are defined on the coordinate range (see section 3) $0 \leqslant \theta \leqslant \pi$, $0 \leqslant R \leqslant \infty$, so that the classical SOS is folded into the interval $0 \leqslant \theta \leqslant \pi$, using the invariance under the transformation $\psi \rightarrow 2\pi - \psi$, $p_\psi \rightarrow -p_\psi$.

Classical SOS for four different energies corresponding to particular eigenstates are shown in figs. 2a (state 24, $E = 2586.83$ cm$^{-1}$), 3a (state 32, $E = 2875.56$ cm$^{-1}$), 4a (state 71, $E = 4019.99$ cm$^{-1}$), and 5a (state 88, $E = 4367.01$ cm$^{-1}$), respectively. By defining the SOS along the isomerization path, the classical dynamics of nonrigid LiCN is exposed very clearly. At low energies, only the LiNC well is accessible (right-hand side of the SOS). At higher energies, the LiCN well becomes accessible (left-hand side of SOS). For energies corresponding to states 71 and 88, isomerization is classically allowed.

Configuration space trajectory plots in ($R$, $\theta$) coordinates, with $\theta$ folded into the interval $0 \leqslant \theta \leqslant \pi$, have also been made [39].

## 3. Quantum mechanics of LiNC/LiCN

Rotationless ($J = 0$) vibrational eigenstates for the quantum version of Hamiltonian (3) are calculated using the DVR-DGB program of Bacic and Light [32]. This method has been described in detail by Bacic et al. [40], and is not reviewed here. 416 basis states were used in the final diagonalization, and eigenvalues converged to within 0.01 cm$^{-1}$ of previously published values [31,32].

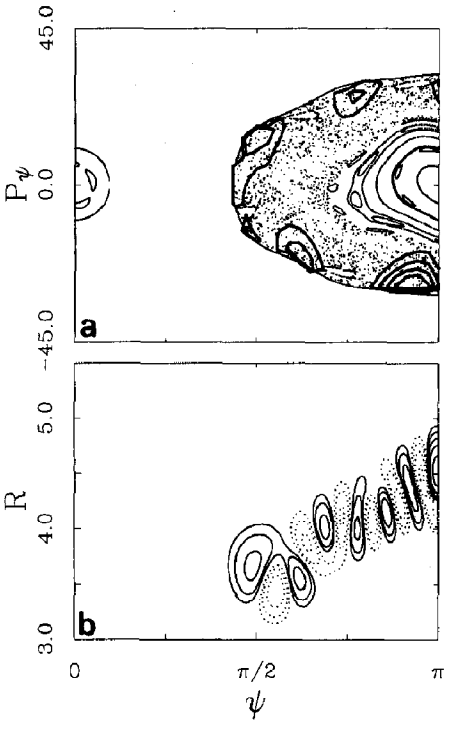


Fig. 2. (a) Classical surface of section for $E = 2586.83$ cm$^{-1}$, the energy of eigenstate 24. Canonical variables ($\psi$, $p_\psi$) are plotted for $\rho = R - R_e(\theta) = 0$. The right-hand side of the surface of section is the region of phase space associated with the LiNC isomer, the left-hand side with the LiCN isomer. The quantum surface of section for $E = 2586.83$ cm$^{-1}$ is superimposed. Contours of a section through the Husimi function of state 24, corresponding to the classical surface of section, are plotted as thick solid lines. (b) Contour plot of the configuration space wavefunction $\psi(R, \theta)$ for state 24.

The wavefunctions in DVR form have been transformed to continuous functions of coordinates ($R$, $\theta$):

$$\psi(R, \theta) = \sum_{\lambda=0}^{45} f_\lambda(R)\, P_\lambda(\cos\theta) , \quad (5)$$

where $0 \leqslant \theta \leqslant \pi$, $0 \leqslant R \leqslant \infty$. We have plotted the first 100 wavefunctions in ($R$, $\theta$) space, and have verified that our functions are very similar in appearance to those shown by FT calculated using a different method [31]. Wavefunction contour plots for eigenstates 24, 32, 71 and 88 are given in figs. 2b, 3b, 4b, and 5b, respectively.

It is very important to note that the wavefunctions

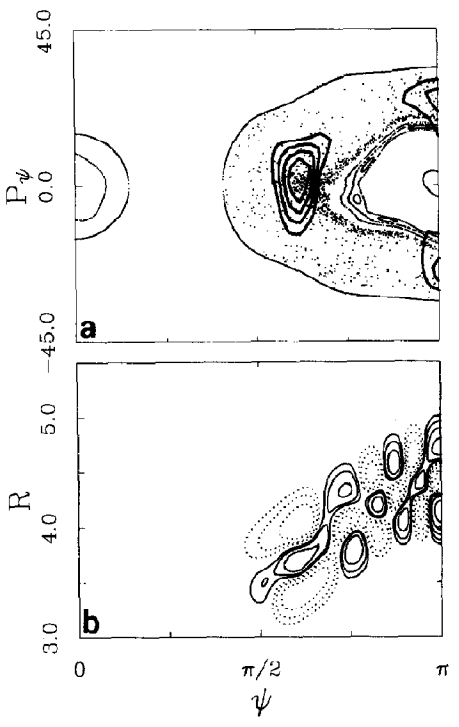


Fig. 3. As for fig. 2, with $E=2875.56\ cm^{-1}$, state 32.

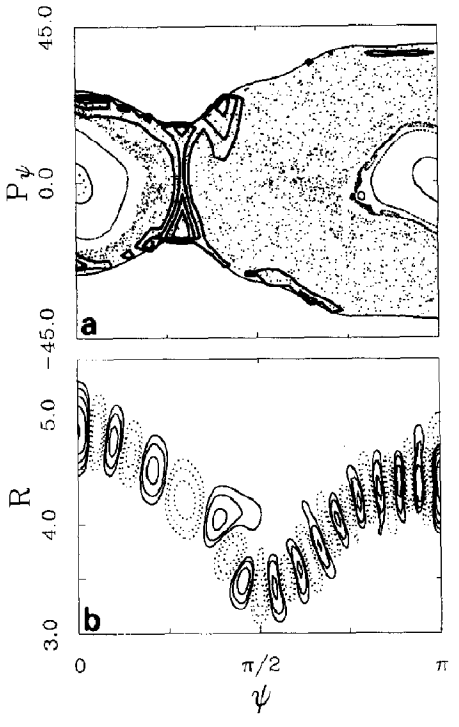


Fig. 4. As for fig. 2, with $E=4019.99\ cm^{-1}$, state 71.

$\psi(R, \theta)$ are normalized with a weight function $R^2 \sin\theta$, appropriate for three-dimensional spherical polar coordinates. The wavefunctions $\psi$ are most usefully thought of as functions of three coordinates, $(R, \theta, \phi)$, where $\phi$ is a second angular coordinate describing rotation of Li around the CN axis, *which happen to be independent of the coordinate* $\phi$. The quantum solutions are inherently three-dimensional, and the restriction of the angle $\theta$ to the interval $0 \leqslant \theta \leqslant \pi$ in the classical SOS defined in section 2 reflects this fact.

The appropriate arena for comparison of classical and quantum mechanics is phase space. To define a phase space representation for the eigenstates of LiCN, we use the Husimi [41] or coherent state [42] representation. Here, the square magnitude of the overlap of the eigenstate $\psi(R, \theta)$ with a coherent state $|\alpha\rangle$ [42] parametrized by a set of phase space coordinates $\alpha$ defines a nonnegative phase space density, sections through which can be regarded as the quantum analogue of the classical SOS [43].

For the nonrigid molecule LiCN/LiNC, in which the bend and stretch frequencies are quite different, there is no obvious or unique way to define a set of coherent states with which to calculate the Husimi function. In the present work, we use isotropic harmonic oscillator coherent states, with width parameter corresponding to the geometric mean of that for the LiNC bend and the LiNC/CN stretch modes [39]. An obvious problem in defining the Husimi function arises from the fact that the wavefunctions $\psi(R, \theta)$ are defined on a half-plane, whereas 2D oscillator coherent states are defined on the full $(x, y)$ plane. It is therefore essential to embed the 2D quantum wavefunction in a three-dimensional Cartesian space, and calculate overlaps between wavefunctions $\psi(R, \theta, \phi)$ (*independent* of angle $\phi$) and 3D harmonic oscillator coherent states centered on the 2D $(R, \theta)$ plane ($\phi$ constant) with zero momentum out of the plane. The three-dimensional integrals required are performed by numerical quadrature [39]. A well defined nonnegative quantum phase space density is thereby obtained.

Quantum surfaces of section [43] (that is, con-

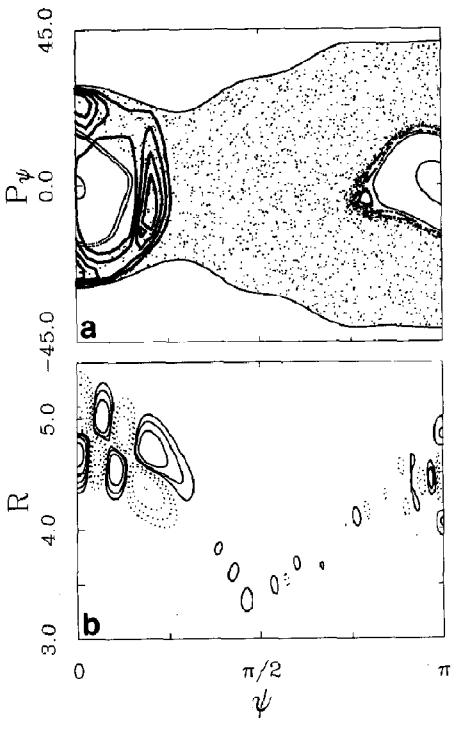


Fig. 5. As for fig. 2, with $E=4367.01$ cm$^{-1}$, state 88.

tour plots of a particular section through the Husimi function) defined in a fashion analogous to the classical SOS of section 2 are superimposed on the corresponding classical SOS in figs. 2a, 3a, 4a and 5a, respectively. Contours of the Husimi function sections are drawn with a thick solid line, to distinguish them from, e.g. islands in the classical SOS.

The task of comparing rotationless ($J=0$) classical and quantum mechanics would be considerably simplified if a planar quantum Hamiltonian were to be used, with the $\theta$ coordinate describing motion of a particle on a ring. The DVR-DGB program of Bacic and Light used to calculate the quantum states treated here employs the full three-dimensional Hamiltonian, however, necessitating the relatively complicated procedures discussed above.

## 4. Comparison of classical and quantum phase space structure

In this section we compare the classical and quantum SOS for several representative states of LiCN. More extensive discussion will be given elsewhere, as will a more detailed examination of the classical mechanics [39].

*State 24.* The classical SOS, quantum SOS, and configuration space wavefunction are shown in fig. 2. The quantum phase space density is highly localized, and lies in a region of phase space that is classically chaotic (fig. 2a). Note that, although small resonant islands are apparent in the stochastic region of the classical SOS, the quantum phase space density is not localized in the vicinity of these islands, but rather between the islands, presumably in the vicinity of the associated unstable periodic orbit. The nodal pattern for this state is not particularly "irregular" [31] (cf. fig. 2b). States 29, 44, 50, 62, 69 and 77 are also of this type.

*State 32.* The classical SOS at the energy of eigenstate 32 shows widespread stochasticity (fig. 3a). Nevertheless, the wavefunction has a quite "regular" nodal pattern, and the quantum phase space density occupies a very compact region in the midst of the large classically chaotic region. The quantum phase space density sits at the leftmost tip of a dark area of the classical chaotic region; such a darkening is indicative of the presence of a phase space bottleneck, which we suspect is associated with the stable and unstable manifolds of a periodic orbit lying along a ridge in the potential analogous to that noted by Smith and Shirts in HCN [44]. This point is currently under investigation. States 30, 48, 53 and 75 are also of this type.

*State 71.* This state was classified as a regular free rotor state by FT [31]. The wavefunction for state 71 is delocalized and indeed has a "regular" nodal pattern (fig. 4b). The corresponding classical SOS reveals global stochasticity (fig. 4a), while the quantum phase space density is localized at the periphery of the classically irregular region. Construction of the stable and unstable manifolds of the unstable periodic orbit located at the top of the isomerization barrier shows that the quantum phase space density for state 71 is localized outside the separatrix manifolds forming the boundaries of both the LiNC and LiCN isomers [39]. States 67, 70, 74, 78 and 82 are also of this type. State 65 is a so-called separatrix state [19]; that is, the phase space density is localized along the separatrix manifolds emanating from the

periodic orbit at the top of the isomerization barrier.

*State 88.* This state is localized in the LiCN well. The wavefunction has a very regular nodal pattern (fig. 5b). The quantum phase space density is nevertheless localized at the edge of the chaotic region of classical phase space (fig. 5a). States 58 and 76 are also of this type.

## 5. Discussion and conclusions

We have compared the classical and quantum phase space structure of a two-mode model of the nonrigid molecule LiNC/LiCN. The quantum phase space densities for many vibrational eigenstates of the LiCN molecule are localized in regions of phase space that are classically completely chaotic. In this limited sense, we do not find any direct qualitative correspondence between the classical and quantum mechanics of LiCN [31]. Moreover, eigenstates with apparently complicated or "irregular" configuration space nodal patterns [31] often have very localized quantum mechanical phase space densities [45] (for example, state number 50, not shown here).

Nonetheless, classical objects such as separatrix manifolds clearly have a profound influence on the quantum phase space density [19]. Further understanding of the relation between the quantum and classical phase space structure of LiCN requires a detailed study of the classical phase space, and such a study is now in progress [39].

## Acknowledgement

This work was supported by NSF Grant CHE-8704632. RMB and FB acknowledge the support of the Comunidad Autonoma de Madrid and CICYT, Spain (contracts PB86/540 and PB87/112). We are very grateful to Z. Bacic and J. Light for providing a version of their DVR-DGB code, and to J. Tennyson for providing a potential subroutine. Computations reported here were performed in part on the Cornell National Supercomputer Facility, which is supported by the NSF and IBM corporation.

## References

[1] A.J. Lichtenberg and M.A. Lieberman, Regular and stochastic motion (Springer, Berlin, 1983);
R.S. MacKay and J.D. Meiss, Hamiltonian dynamical systems (Hilger, Bristol, 1986);
A.M. Ozorio de Almeida, Hamiltonian systems: chaos and quantization (Cambridge Univ. Press, Cambridge, 1988).
[2] R.S. MacKay, J.D. Meiss and I.C. Percival, Physica D 13 (1984) 55.
[3] D. Bensimon and L.P. Kadanoff, Physica D 13 (1984) 82.
[4] S.R. Channon and J. Lebowitz, Ann. NY Acad. Sci. 357 (1980) 108.
[5] R.S. MacKay, J.D. Meiss and I.C. Percival, Physica D 27 (1987) 1.
[6] M.J. Davis, J. Chem. Phys. 83 (1985) 1016.
[7] S.K. Gray and S.A. Rice, J. Chem. Phys. 86 (1987) 2020.
[8] M.J. Davis and S.K. Gray, J. Chem. Phys. 84 (1986) 5389.
[9] S.K. Gray, S.A. Rice and M.J. Davis, J. Phys. Chem. 90 (1986) 3470.
[10] S.K. Gray and S.A. Rice, Faraday Discussions Chem. Soc. 82 (1987) 307.
[11] M.J. Davis, J. Chem. Phys. 86 (1987) 3978.
[12] R.T. Skodje and M.J. Davis, J. Chem. Phys. 88 (1988) 2429.
[13] J.D. Meiss and E. Ott, Physica D 20 (1986) 387.
[14] C.C. Martens, M.J. Davis and G.S. Ezra, Chem. Phys. Letters 142 (1987) 519; to be submitted for publication.
[15] S.H. Tersigni and S.A. Rice, Bericht. Bunserges. Physik. Chem. 92 (1988) 209.
[16] R.E. Gillilan and W.P. Reinhardt, Chem. Phys. Letters 156 (1989) 478.
[17] S. Wiggins, preprint.
[18] B. Eckhardt, Phys. Rept. 163 (1988) 205.
[19] M.J. Davis, J. Phys. Chem. 92 (1988) 3124.
[20] E.J. Heller and R.L. Sundberg, in: Proceedings of the NATO Conference on Quantum Chaos, ed. G. Casati (Plenum Press, New York, 1983);
E.J. Heller, Phys. Rev. Letters 53 (1984) 1515; Lecture notes in physics, Vol. 263 (Springer, Berlin, 1986) p. 162;
P.W. O'Connor and E.J. Heller, Phys. Rev. Letters 61 (1988) 2288.
[21] R.C. Brown and R.E. Wyatt, Phys. Rev. Letters 57 (1986) 1; J. Phys. Chem. 90 (1986) 3590;
R.S. MacKay and J.D. Meiss, Phys. Rev. A 37 (1988) 4702.
[22] T. Geisel, G. Radons and J. Rubner, Phys. Rev. Letters 57 (1986) 2883;
G. Radons, T. Geisel and J. Rubner, Advan. Chem. Phys. 73 (1989) 891.
[23] L.L. Gibson, G.C. Schatz, M.A. Ratner and M.J. Davis, J. Chem. Phys. 86 (1987) 3263.
[24] R.L. Waterland, J.-M. Yuan, C.C. Martens, R.E. Gillilan and W.P. Reinhardt, Phys. Rev. Letters 61 (1988) 2733.
[25] G. Radons and R.E. Prange, Phys. Rev. Letters 61 (1988) 1691.

[26] M. Founargiotakis, S.C. Farantos and J. Tennyson, J. Chem. Phys. 88 (1988) 1598;
M. Founargiotakis, S.C. Farantos, G. Contopoulos and C. Poulimis, preprint;
S.C. Farantos, M. Founargiotakis and C. Poulimis, preprint.
[27] C.C. Martens, J. Chem. Phys., in press.
[28] H.S. Taylor, J. Zakrzewski and S. Saini, Chem. Phys. Letters, 145 (1988) 555.
[29] J.M. Gomez-Llorente, J. Zakrzewski, H.S. Taylor and K.C. Kulander, J. Chem. Phys. 90 (1989) 1505.
[30] E.B. Bogomolny, Physica D 31 (1988) 169.
[31] S.C. Farantos and J. Tennyson, J. Chem. Phys. 82 (1985) 800;
J. Tennyson and S.C. Farantos, Chem. Phys. Letters 109 (1984) 160; Chem. Phys. 93 (1985) 237;
J. Tennyson, G. Brocks and S.C. Farantos, Chem. Phys. 104 (1986) 399.
[32] Z. Bacic and J.C. Light, J. Chem. Phys. 85 (1986) 4595.
[33] R. Essers, J. Tennyson and P.E.S. Wormer, Chem. Phys. Letters 89 (1982) 223;
G. Brocks, J. Tennyson and A. vand der Avoird, J. Chem. Phys. 80 (1984) 3223.
[34] R.M. Stratt, N.C. Handy and W.H. Miller, J. Chem. Phys. 71 (1979) 3311.
[35] M.V. Berry, in: Chaotic behavior of deterministic systems, eds. G. Looss, R. Helleman and R. Stora (North-Holland, Amsterdam, 1983).
[36] N. Pomphrey, J. Phys. B 7 (1974) 1909.
[37] D.W. Noid, M.L. Koszykowski and R.A. Marcus, Chem. Phys. Letters 73 (1980) 269;
D.W. Noid, M.L. Koszykowski, M. Tabor and R.A. Marcus, J. Chem. Phys. 72 (1980) 6169.
[38] G. Benettin, L. Galgani and J.-M. Strelcyn, Phys. Rev. A 14 (1976) 2338.
[39] R.M. Benito, F. Borondo, J.-H. Kim and G.S. Ezra, in preparation.
[40] Z. Bacic, R.M. Whitnell, D. Brown and J.C. Light, Computer Phys. Commun. 51 (1988) 35;
Z. Bacic and J.C. Light, Ann. Rev. Phys. Chem., in press.
[41] K. Husimi, Proc. Phys. Math. Soc. Japan 22 (1940) 264;
K. Takahashi, J. Phys. Soc. Japan 55 (1986) 762.
[42] J. Klauder and E.C.G. Sudarshan, Fundamentals of quantum optics (Benjamin, New York, 1968);
S.W. McDonald, Phys. Rept. 158 (1988) 337.
[43] J.S. Hutchinson and R.E. Wyatt, Chem. Phys. Letters 72 (1980) 378;
Y. Weissman and J. Jortner, J. Chem. Phys. 77 (1982) 1486.
[44] R.S. Smith and R.B. Shirts, J. Chem. Phys. 89 (1988) 2949.
[45] N. DeLeon, M.J. Davis and E.J. Heller, J. Chem. Phys. 80 (1984) 794.